This article was downloaded by: [Renmin University of China]
On: 13 October 2013, At: 10:30
Publisher: Taylor & Francis
Informa Ltd Registered in England and Wales Registered Number: 1072954 Registered office: Mortimer House, 37-41 Mortimer Street, London W1T 3JH, UK

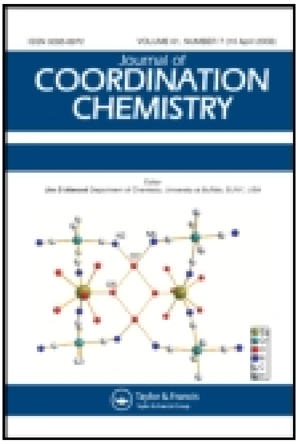

Journal of Coordination Chemistry
Publication details, including instructions for authors and subscription information:
http://www.tandfonline.com/loi/gcoo20

Template synthesis and spectral characterization of some Schiff base complexes derived from quinoxaline-2-carboxaldehyde and L-histidine

Manju Sebastian [a] , Vasudevan Arun [a] , Ponminiessary P. Robinson [a] , Pally Leeju [a] , Gopalakrishnan Varsha [a] , Digna Varghese [a] & Karukapadath K. Mohammed Yusuff [a]

[a] Department of Applied Chemistry , Cochin University of Science and Technology , Cochin - 682022, Kerala, India

Published online: 18 Jan 2011.

To cite this article: Manju Sebastian , Vasudevan Arun , Ponminiessary P. Robinson , Pally Leeju , Gopalakrishnan Varsha , Digna Varghese & Karukapadath K. Mohammed Yusuff (2011) Template synthesis and spectral characterization of some Schiff base complexes derived from quinoxaline-2-carboxaldehyde and L-histidine, Journal of Coordination Chemistry, 64:3, 525-533, DOI: 10.1080/00958972.2010.549940

To link to this article: http://dx.doi.org/10.1080/00958972.2010.549940

PLEASE SCROLL DOWN FOR ARTICLE

Taylor & Francis makes every effort to ensure the accuracy of all the information (the "Content") contained in the publications on our platform. However, Taylor & Francis, our agents, and our licensors make no representations or warranties whatsoever as to the accuracy, completeness, or suitability for any purpose of the Content. Any opinions and views expressed in this publication are the opinions and views of the authors, and are not the views of or endorsed by Taylor & Francis. The accuracy of the Content should not be relied upon and should be independently verified with primary sources of information. Taylor and Francis shall not be liable for any losses, actions, claims, proceedings, demands, costs, expenses, damages, and other liabilities whatsoever or howsoever caused arising directly or indirectly in connection with, in relation to or arising out of the use of the Content.

This article may be used for research, teaching, and private study purposes. Any substantial or systematic reproduction, redistribution, reselling, loan, sub-licensing, systematic supply, or distribution in any form to anyone is expressly forbidden. Terms &

Journal of Coordination Chemistry
Vol. 64, No. 3, 10 February 2011, 525–533

Template synthesis and spectral characterization of some Schiff base complexes derived from quinoxaline-2-carboxaldehyde and L-histidine

MANJU SEBASTIAN, VASUDEVAN ARUN, PONMINIESSARY P. ROBINSON, PALLY LEEJU, GOPALAKRISHNAN VARSHA, DIGNA VARGHESE and KARUKAPADATH K. MOHAMMED YUSUFF*

Department of Applied Chemistry, Cochin University of Science and Technology,
Cochin – 682022, Kerala, India

(*Received 20 February 2010; in final form 5 November 2010*)

New Schiff base complexes of Mn(II), Fe(III), Co(II), Ni(II), Cu(II), and Zn(II) were synthesized by template condensation of quinoxaline-2-carboxaldehyde, L-histidine, and the metal compound, and were characterized by elemental analysis, fourier transform infrared spectroscopy, electronic spectra, conductance measurements, magnetic susceptibility measurements, ESR spectra, and thermal analysis. In all the complexes, the Schiff base coordinates through azomethine nitrogen, quinoxaline nitrogen, and carboxylato oxygen. The physico-chemical and spectroscopic measurements reveal square planar geometry for the copper(II) complex, tetrahedral geometry for the manganese(II), cobalt(II), and zinc(II) complexes, and octahedral geometry for the iron(III) and nickel(II) complexes.

Keywords: Schiff base complex; Template method; Quinoxaline-2-carboxaldehyde; L-histidine; Amino acid

1. Introduction

Schiff bases are used for synthesis of metal complexes due to their easy formation and strong metal-binding ability. Schiff bases and their complexes have wide applications [1–4]. Amino acid Schiff base complexes have catalytic, pharmacological, and biological properties [5–7], and are considered as good models to study metal–ligand interactions in metalloproteins and metalloenzymes [8, 9]. It was thought worthwhile to synthesize complexes of the Schiff base derived from the amino acid, L-histidine, which itself serves as a ligand through the imidazole imido nitrogen in many enzymes. As we could not isolate the free Schiff base, we have adopted a template method for the synthesis of its complexes. A large number of reports have appeared on template synthesis of metal complexes [10–15]. The template synthesis and characterization of transition metal complexes of the Schiff base derived from glycine and quinoxaline-2-carboxaldehyde [16] were already reported. In continuation of that work, we present here the template

---

*Corresponding author. Email: yusuff@cusat.ac.in

Journal of Coordination Chemistry
ISSN 0095-8972 print/ISSN 1029-0389 online © 2011 Taylor & Francis
DOI: 10.1080/00958972.2010.549940

synthesis and characterization of manganese(II), iron(III), cobalt(II), nickel(II), copper(II), and zinc(II) complexes of a Schiff base derived from quinoxaline-2-carboxaldehyde and L-histidine. The Schiff base quinoxaline-2-carboxalidine—L-histidine is abbreviated as HL.

2. Experimental

2.1. *Materials and physical measurements*

L-Histidine (Aldrich), manganese(II) acetate tetrahydrate (Merck), anhydrous ferric chloride (Merck), cobalt(II) acetate tetrahydrate (Qualigens), nickel(II) acetate tetrahydrate (Qualigens), copper(II) chloride dihydrate (Merck), and zinc(II) acetate dihydrate (Merck) are used as supplied. Preparation of quinoxaline-2-carboxaldehyde was carried out as reported in the literature [17, 18].

Elemental analyses of the complexes were done on a Vario EL III CHNS analyser. The estimation of metal ions was carried out on a Thermo Electron Corporation, M series Atomic Absorption Spectrophotometer. Estimation of chloride was carried out by Volhard's method. The ^{1}H-NMR spectrum was recorded in $CDCl_3$ or DMSO-d_6 on a Bruker AVAVCE III 400 MHz NMR spectrometer using TMS as the internal standard. Molar conductance of the complexes in DMF (10^{-3} mol) was measured at 298 K with a Systronic model 303 direct-reading conductivity bridge. Magnetic susceptibility measurements were done at room temperature on a Magway MSB Mk 1 Magnetic Susceptibility Balance. IR spectra were recorded on a JASCO FTIR-4100 spectrometer using KBr pellets in the range 400–4000 cm^{-1}. Electronic spectra of the complexes were recorded on a Thermoelectron Nicolet evolution 300 UV-Vis spectrophotometer. Thermo gravimetry–differential thermal analyser (TG—DTA) analyses were carried out on a Perkin Elmer Pyris Diamond TG/DTA analyser. Electron paramagnetic resonance (EPR) spectra of the complexes were recorded on a Varian E-112 spectrometer using TCNE as the standard.

2.2. *Synthesis of complexes of HL*

Quinoxaline-2-carboxaldehyde (1.58 g, 10 mmol) was dissolved in methanol (50 mL) and added to an aqueous solution of L-histidine (1.55 g, 10 mmol in 30 mL water). The solution was then refluxed on a water bath for 30 min. The color of the solution darkens, indicating formation of the Schiff base. To this, 10 mmol of the metal compound (1.98 g of manganese chloride tetrahydrate, 1.62 g of ferric chloride anhydrous, 2.38 g of cobalt chloride tetrahydrate, 2.37 g of nickel chloride hexahydrate, 1.70 g of copper chloride dihydrate, or 2.19 g of zinc acetate dihydrate) in 15 mL methanol was added. The solution was again refluxed for 3 h. The progress of the formation of the metal complex was monitored by thin layer chromatography. The complex separated on keeping the solution at room temperature; it was filtered and washed with 1 : 1 methanol–water solution and then with acetone. Figure 1 gives the general scheme of formation of the complexes of HL.

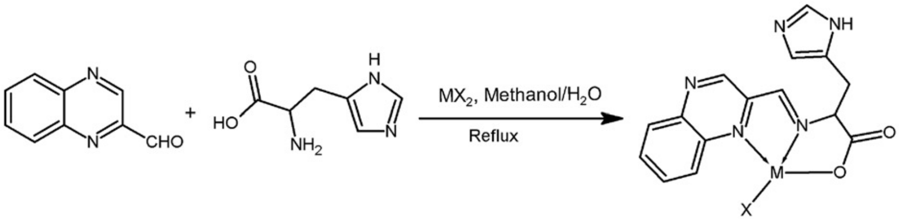

Figure 1. The general scheme of formation of complexes of HL.
Note: MX$_2$, M is the metal ion and X is the anion.

[MnL(OAc)]·2H$_2$O – Yield: 55%, Color: brown, λ_m (DMF): 7 Ohm^{-1} cm^2 mol^{-1}, Elemental Anal. Calcd for $C_{17}H_{19}MnN_5O_6$ (444.3): C, 45.96; H, 4.31; N, 15.76; and Mn, 12.37. Found: C, 46.07; H, 4.25; N, 15.41; and Mn, 12.31%.

[FeLCl$_2$(H$_2$O)]·H$_2$O – Yield: 70%, Color: black, λ_m (DMF): 15 Ohm^{-1} cm^2 mol^{-1}, Elemental Anal. Calcd for $C_{15}H_{16}Cl_2FeN_5O_4$ (457.1): C, 39.42; H, 3.53; N, 15.32; Fe, 12.22; and Cl, 15.51. Found: C, 40.05; H, 2.98; N, 15.41; Fe, 12.11; and Cl, 15.73%.

[CoL(OAc)]·2H$_2$O – Yield: 62%, Color: black, λ_m (DMF): 11 Ohm^{-1} cm^2 mol^{-1}, Elemental Anal. Calcd for $C_{17}H_{19}CoN_5O_6$ (448.3): C, 45.55; H, 4.27; N, 15.62; and Co, 13.15. Found: C, 45.51; H, 3.97; N, 15.62; and Co, 13.14%.

[NiL(OAc)(H$_2$O)$_2$]·H$_2$O – Yield: 65%, Color: black, λ_m (DMF): 18 Ohm^{-1} cm^2 mol^{-1}, Elemental Anal. Calcd for $C_{17}H_{21}NiN_5O_7$ (466.1): C, 43.81; H, 4.54; N, 15.03; and Ni, 12.59. Found: C, 43.42; H, 4.69; N, 15.19; and Ni, 12.81%.

[CuLCl]·2H$_2$O – Yield: 72%, Color: brown, λ_m (DMF): 9 Ohm^{-1} cm^2 mol^{-1}, Elemental Anal. Calcd for $C_{15}H_{16}ClCuN_5O_5$ (429.3): C, 41.96; H, 3.76; N, 16.31; Cu, 14.80; and Cl, 8.26. Found: C, 41.54; H, 3.32; N, 16.36; Cu, 15.09; and Cl, 8.45%.

[ZnL(OAc)]·2H$_2$O – Yield: 70%, Color: red, λ_m (DMF): 5 Ohm^{-1} cm^2 mol^{-1}, Elemental Anal. Calcd for $C_{17}H_{19}ZnN_5O_6$ (454.5): C, 44.90; H, 4.21; N, 15.40; and Zn, 14.38. Found: C, 44.87; H, 4.09; N, 15.48; and Zn, 14.47%.

3. Results and discussion

Analytical data calculated for the complexes reveal a metal-to-ligand ratio of 1 : 1 for all the complexes. All the complexes in DMF (10^{-3} mol L^{-1} solution) exhibit molar conductance values of 5–25 Ohm^{-1} cm^2 mol^{-1}, suggesting the non-electrolytic nature of the complexes [19] and the binding of the anions to the metal.

3.1. *NMR spectrum of [ZnL(OAc)]·2H$_2$O*

^{1}H-NMR spectral data of the zinc(II) complex in DMSO-d$_6$ confirm the proposed structure of the ligand in complexes. The proton NMR spectrum of zinc(II) complex was taken in d$_6$-DMSO (Supplementary materials). The N–H proton resonates at

Table 1. IR spectral data of the complexes of HL.

Assignments	$\nu(H_2O)$, $\nu(NH)$	$\nu(COO^-)$ asym	$\nu(COO^-)$ sym	Δ	$\nu(C{=}N)$ azomethine	ν(M–O)	ν(M–N)
$[MnL(OAc)] \cdot 2H_2O$	3330 b	1652	1416	236	1613	446	409
$[FeLCl_2H_2O] \cdot 2H_2O$	3300 b	1640	1412	228	1617	440	414
$[CoL(OAc)] \cdot 2H_2O$	3300 b	1645	1409	236	1613	442	416
$[NiL(OAc)(H_2O)_2] \cdot H_2O$	3397, 3361	1650	1407	243	1613	440	420
$[CuLCl] \cdot 2H_2O$	3505, 3421	1642	1404	238	1621	435	413
$[ZnL(OAc)] \cdot 2H_2O$	3300 b	1653	1417	236	1621	446	415

b, broad; $\Delta = \nu(COO^-)$ asymmetric; and $\nu(COO^-)$ symmetric.

8.75 ppm, which is comparable to the reported value of histidine NH [20] in the spectrum of peptide containing histidine, where the histidine NH resonates at 8.4 ppm [21]. Water appears as a broad signal at 3.9–4.3 ppm and the aromatic protons appear as a multiplet at 7.60–8.50 ppm. The signal due to azomethine –CH proton occurs as a singlet at 9.45 ppm, in the range expected for azomethines [22–25]. Signals at 6.80–7.00 ppm and 2.08 ppm can be attributed to imidazole and acetate, respectively. Singlets at 2.70 ppm and 2.90 ppm are due to protons at carbons α and β to the amino and carboxyl moieties. These observations clearly suggest the formation of the Schiff base complex.

3.2. *Infrared spectra*

Infrared (IR) spectral data of the most relevant bands are presented in table 1. As we were not able to isolate the free ligand, the assignments of the IR bands of the complexes are done based on the IR spectra of the histidine and quinoxaline-2-carboxaldehyde. Most of the bands due to the histidine and quinoxaline-2-carboxaldehyde are present in spectra of the complexes. However, the C=O stretching observed in quinoxaline-2-carboxaldehyde at 1680 cm^{-1} is absent in spectra of complexes, confirming the formation of Schiff base. IR spectral bands at 1610–1660 cm^{-1} are attributable to asymmetric stretching of $\nu(COO^-)$ and $\nu(C{=}N)$ of the azomethine [26]. For acetato complexes, $\nu(COO^-)$ appears as a sharp band at 1650 cm^{-1}. However, it appears that this sharp band masks the $\nu(COO^-)$ of the Schiff base. The symmetric $\nu(COO^-)$ is observed at 1400–1420 cm^{-1} [27]. In the spectra of all the complexes, the separation between $\nu(COO^-)$ asymmetric and $\nu(COO^-)$ symmetric bands is 230–240 cm^{-1}, indicating monodentate coordination [26]. All the complexes show a broad absorption at 3300 cm^{-1}, indicating water. The presence of coordinated water in the iron(III) and the nickel(II) complex are confirmed by the sharp bending vibrational band at 750–800 cm^{-1} [26]. The (N–H) stretching of imidazole also occurs in this region. Due to this overlap, the bands could not be differentiated. The (C=N) stretch of quinoxaline occurs at 1550–1590 cm^{-1} [28]. The low-frequency vibrations observed around 400 cm^{-1} are due to metal–nitrogen and metal–oxygen stretches.

3.3. *Electronic absorption spectra and magnetic susceptibility measurements*

The UV-Vis spectra of the Schiff base complexes in methanol (figure 2) are listed in table 2 with absorption maxima and magnetic moments. Bands observed above

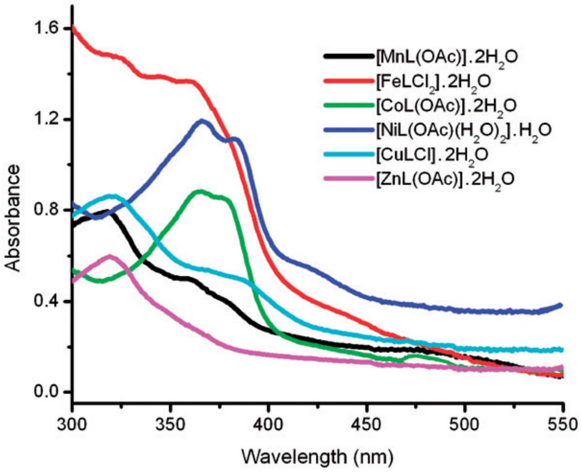

Figure 2. The electronic spectra of the complexes in methanol (wavelength range is limited between 300–550 nm for ease in viewing d–d bands).

Table 2. Magnetic moments and UV-Vis spectral data.

Compound	Absorption maxima[a] (log ε)	μ_{eff} (B.M)
$[MnL(OAc)] \cdot 2H_2O$	42,000(3.36), 31,450(2.89), 27,850(2.08), 20,200(1.90)	5.96
$[FeLCl_2(H_2O)] \cdot H_2O$	41,600(3.72), 31,050(3.23), 27,700(3.20), 22,400(1.95)	5.83
$[CoL(OAc)] \cdot 2H_2O$	40,000(3.61), 27,400(3.37), 21,000(3.14), 10,800(1.95)	4.66
$[NiL(OAc)(H_2O)_2] \cdot H_2O$	39,840(3.53), 27,320(3.27), 23,580(1.60), 17,760(1.48), 9780(0.97)	3.32
$[CuLCl] \cdot 2H_2O$	41,660(3.75), 31,340(3.33), 25,900(2.47), 15,540(1.90)	1.92
$[ZnL(OAc)] \cdot 2H_2O$	42,190(3.63), 31,250(3.24)	–

[a] Absorption maxima in cm^{-1} and ε in L mol^{-1} cm^{-1}.

28,500 cm^{-1} are identical and assigned to π–π* transitions and intraligand charge transfer transitions of the quinoxaline ring, imidazole ring, and azomethine C=N. The forbidden $n-\pi^*$ transitions are not noticeable.

Spectra of tetrahedral manganese(II) complexes usually exhibit bands at 19,000–25,000 cm^{-1}, 25,000–29,000 cm^{-1}, and 35,000–38,000 cm^{-1} [29]. Also, $[MnL(OAc)] \cdot 2H_2O$ exhibits bands at 27,850 and 20,200 cm^{-1}, indicating tetrahedral manganese. The μ_{eff} value of $[MnL(OAc)] \cdot 2H_2O$ was found to be 5.96 B.M. at room temperature, as expected for a high spin d^5 system (table 2) [30].

The four lowest energy bands expected for high-spin octahedral iron (III) complexes are the transition from the ground state $^6A_{1g}$ to $^4T_{1g}$, $^4T_{2g}$, ^4E_g, and $^4A_{1g}$ excited states. $[FeLCl_2(H_2O)] \cdot H_2O$ exhibits only a charge transfer band at 27,700 and a weak shoulder at 22,400 cm^{-1}. The shoulder band might be due to the $^6A_{1g} \rightarrow {}^4T_{1g}$ transition expected for the iron(III) octahedral complexes [31]. The charge transfer band might have obscured the forbidden d–d transitions. The magnetic moment of the iron(III) complex is 5.83 B.M. [30].

The room temperature magnetic moment of $[CoL(OAc)] \cdot 2H_2O$ is 4.66 B.M., suggesting a tetrahedral structure [32]. Also, $[CoL(OAc)] \cdot 2H_2O$ exhibits two weak bands at 10,800 and 21,000 cm^{-1}, which correspond to the expected $^4A_2 \rightarrow {}^4T_1(F)$ and

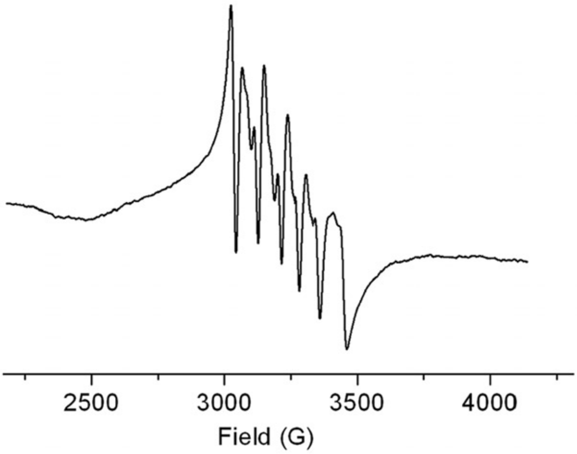

Figure 3. The EPR spectrum of $[MnL(OAc)]\cdot 2H_2O$ at 77 K.

${}^4A_2 \rightarrow {}^4T_1(P)$ transitions of cobalt(II) tetrahedral complexes [29]. The ${}^4A_2 \rightarrow {}^4T_2$ transition is not observed.

The magnetic moment of $[NiL(OAc)(H_2O)_2]\cdot H_2O$ is 3.32 B.M., which indicates an octahedral geometry around nickel [33]. The complex exhibits three d–d transitions at 23,580, 17,760, and 9780 cm^{-1} due to ${}^3A_{2g} \rightarrow {}^3T_{2g}$, ${}^3A_{2g} \rightarrow {}^3T_{1g}$, and ${}^3A_{2g} \rightarrow {}^3T_{1g}(P)$ transitions of octahedral nickel(II).

Complex $[CuLCl]\cdot 2H_2O$ exhibits a broad band in the visible region from 15,540 cm^{-1} assignable to ${}^2B_{1g} \rightarrow {}^2E_g$ transition and also the band at 25,900 cm^{-1} corresponds to ${}^2B_{1g} \rightarrow {}^2A_{1g}$, indicating square planar copper [29, 34]. The magnetic moment of the complex is 1.92 B.M. which shows the lack of Cu–Cu interactions and monomeric nature of the complex. The zinc(II) complex exhibits an intraligand charge transfer transition at 31,250 cm^{-1}.

3.4. *EPR spectra of manganese(II) and copper(II) complexes*

The X-band EPR spectra of the copper(II) and manganese(II) complexes were recorded in polycrystalline state at 298 K and in DMF at 77 K.

The EPR spectrum of the Mn(II) complex in polycrystalline state gives a broad signal with a g value of 2.11. The broad nature of the signal at room temperature is due to dipolar interactions and enhanced spin-lattice relaxation. The EPR spectrum of the manganese(II) complex at 77 K exhibits the expected six lines with g and A of 1.99 and 90G (figure 3).

In polycrystalline state, the copper(II) complex exhibits an isotropic spectrum with a g value of 2.07. The extensive exchange coupling through misalignment of the local molecular axes between different molecules in the unit cell (dipolar broadening) and enhanced spin lattice relaxation make the signal very broadly and this type of spectrum gives no information on the electronic ground state of the Cu(II) ion present in the complexes [35].

The EPR spectrum of the copper(II) complex in DMF at 77 K (figure 4) exhibits two $g_{\parallel}$ values, one at 2.14 and the other at 2.20 and $g_{\perp}$ value at 2.06, which suggests

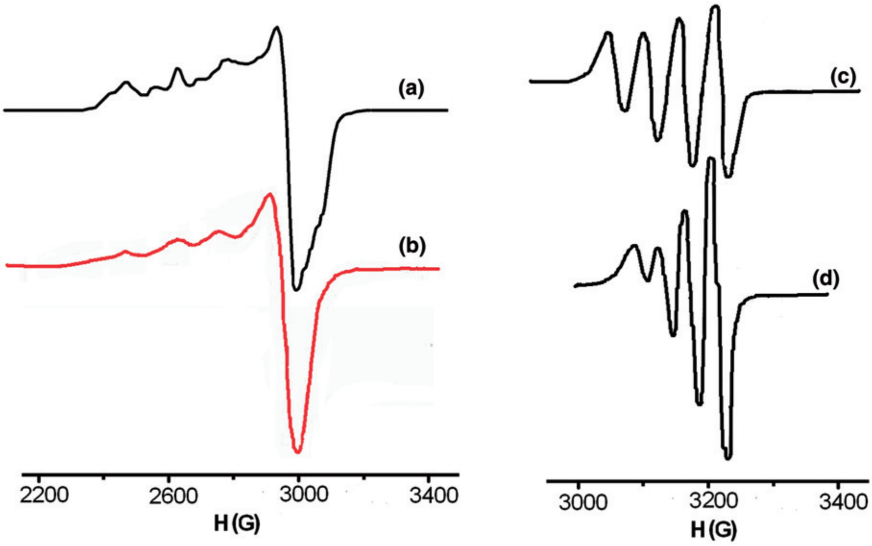

Figure 4. The EPR spectra of $[CuLCl]\cdot 2H_2O$ (a) In DMF at 77 K, (b) In $CHCl_3$ at 77 K, (c) In DMF at 298 K, (d) In $CHCl_3$ at 298 K.

copper(II) in two different environments [36]. An additional environment, different from the square planar environment of [CuLCl], might have been created due to coordinating DMF [37]. To overcome this problem, the spectrum has also been recorded at 298 and 77 K in chloroform. At 77 K, an axial spectrum with a $g_{\parallel}$ value of 2.21 and $g_{\perp}$ value of 2.07 was obtained. The trend $g_{\parallel} > g_{\perp} > g_e$ (g_e is the g value of the free electron, 2.0023) observed for the copper(II) complex shows that the unpaired electron is most likely localized in d_{x^2}–d_{y^2} orbital of the copper(II) and the special features are characteristic of an axial symmetry. At 298 K, EPR spectra of the copper(II) complex are isotropic irrespective of the solvents with four well-resolved hyperfine lines. In DMF, g_{iso} of 2.086 and in chloroform, g_{iso} of 2.099 are obtained.

3.5. *Thermal analysis*

Thermal stabilities of the Schiff base complexes were investigated using TG-DTA under nitrogen with a heating rate of 10°C min^{-1} from 40–1000°C. Weight loss below 120°C in all complexes suggests the presence of lattice water [38]. Similarly, weight loss at 140–210°C in the nickel(II) and iron(III) complexes suggest the presence of coordinated water (table 3). All the complexes are thermally stable and exhibit multistage decomposition. A representative thermogram is given in "Supplementary material". TG results show good agreement with molecular formulas from the analytical data.

4. Conclusions

We have accomplished the facile synthesis of six complexes of the Schiff base quinoxaline-2-carboxalidine–L-histidine by template method and characterized them by

Table 3. Thermogravimetric data of the complexes below 200°C.

Complex	Temperature range (°C)	Loss (%)	Fragment lost	Nature of water lost
$[Mn(qlh)(OAc)] \cdot 2H_2O$	60–120	8.3	$2 \cdot H_2O$	Lattice water
$[Fe(qlh)Cl_2(H_2O)] \cdot H_2O$	55–125	4.1	$1 \cdot H_2O$	Lattice water
	160–210	3.9	$1 \cdot H_2O$	Coordinated water
$[Co(qlh)(OAc)] \cdot H_2O$	60–120	4.3	$1 \cdot H_2O$	Lattice water
$[Ni(qlh)(OAc)(H_2O)_2] \cdot H_2O$	70–132	3.8	$1 \cdot H_2O$	Lattice water
	140–195	7.5	$2 \cdot H_2O$	Coordinated water
$[Cu(qlh)Cl] \cdot 2H_2O$	70–140	8.5	$2 \cdot H_2O$	Lattice water
$[Zn(qlh)(OAc)] \cdot 2H_2O$	50–130	7.9	$2 \cdot H_2O$	Lattice water

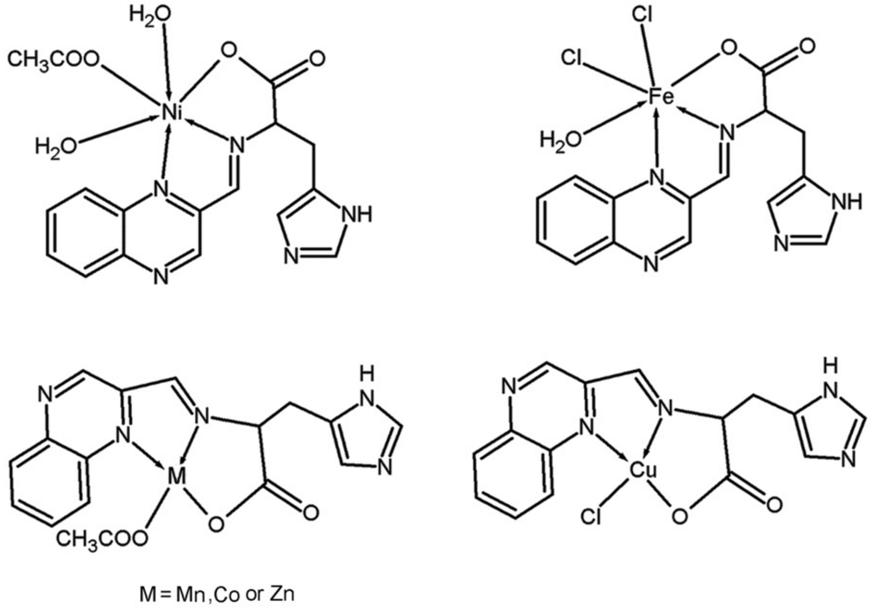

Figure 5. Suggested structures of the complexes of quinoxaline-2-carboxalidine–L-histidine (solvated water molecules are omitted).

elemental analysis, conductivity studies, magnetic susceptibility measurements, IR, UV–Vis, EPR, and thermal studies. Based on these studies, square planar geometry is proposed for the copper(II) complex, octahedral geometry for iron(III) and nickel(II) complexes, and tetrahedral geometry for manganese(II), cobalt(II), and zinc(II) complexes (figure 5). In all complexes, the Schiff base is monobasic tridentate.

Acknowledgments

Manju Sebastian thanks Kerala State Council for Science, Technology and Environment, Kerala and Digna Varghese thanks Council of Scientific and Industrial

Research, India for granting research fellowships. The authors thank Department of Science and Technology, India, for allowing them to use the Sophisticated Analytical Instrumentation Facility (SAIF) at IIT Bombay for the EPR spectral data and at the Sophisticated Test & Instrumentation Centre, Cochin University of Science and Technology for the elemental analyses and NMR spectral analysis.

References

[1] A.D. Garnovskii, I.S. Vasilchenko, D.A. Garnovskii, B.I. Kharisov. *J. Coord. Chem.*, **62**, 151 (2009).
[2] P.G. Cozzi, L.S. Dolci, A. Garelli, M. Montalti, L. Prodi, N. Zaccheroni. *New J. Chem.*, **27**, 692 (2003).
[3] P.A. Vigato, S. Tamburini. *Coord. Chem. Rev.*, **248**, 1717 (2004).
[4] A.D. Garnovskii, A.P. Sadimenko, I.S. Vasilchenko, D.A. Garnovskii, E.V. Sennikova, V.I. Minkin. *Adv. Heterocycl. Chem.*, **97**, 291 (2009).
[5] D. Sinha, A.K. Tiwari, S. Singh, G. Shukla, P. Mishra, H. Chandra, A.K. Mishra. *Eur. J. Med. Chem.*, **43**, 160 (2008).
[6] R.-M. Wang, C.-J. Hao, Y.-P. Wang, S.-B. Li. *J. Mol. Catal. A: Chem.*, **147**, 173 (1999).
[7] M.A. Neelakantan, F. Rusalraj, J. Dharmaraja, S. Johnsonraja, T. Jeyakumar, M.S. Pillai. *Spectrochim. Acta A*, **71**, 1599 (2008).
[8] S.R. Collinson, D.E. Fenton. *Coord. Chem. Rev.*, **148**, 19 (1996).
[9] H.S. He, D.T. Puerta, S.M. Cohen, K.R. Rodgers. *Inorg. Chem.*, **44**, 7431 (2005).
[10] O. Costisor, W. Linert. *Metal Mediated Template Synthesis of Ligands*, p. 24, World Scientific Publishing Company, Singapore (2004).
[11] H. Naeimi, K. Rabiei, F. Salimi. *J. Coord. Chem.*, **62**, 1199 (2009).
[12] V.R. Souza, H.R. Rechenberg, J.A. Bonacin, H.E. Toma. *Spectrochim. Acta A*, **71**, 1296 (2008).
[13] J.I. Gradinaru, S.T. MalinovskiÏ, M.A. Popovici, M. Gdaniec. *Crystallogr. Rep.*, **50**, 217 (2005).
[14] E.H. Charles, L.M.L. Chia, J. Rothery, E.L. Watson, E.J.L. McInnes, R.D. Farley, A.J. Bridgeman, F.E. Mabbs, C.C. Rowlands, M.A. Halcrow. *J. Chem. Soc., Dalton Trans.*, 2087 (1999).
[15] D. Pawlica, M. Marszałek, G. Mynarczuk, L. Sieron, J. Eilmes. *New J. Chem.* , **28**, 1615 (2004).
[16] K.K.M. Yusuff, R. Sreekala. *Synth. React. Inorg. Met. Org. Chem.*, **21**, 553 (1991).
[17] H. Ohle, J.J. Kruyff. *Ber.*, **77B**, 507 (1944).
[18] C.L. Leese, H.N. Rydon. *J. Chem. Soc.*, 303 (1955).
[19] W.J. Geary. *Coord. Chem. Rev.*, **7**, 81 (1971).
[20] I.A. Tolmacheva, I.V. Mashevskaya, A.N. Maslivets. *Russ. J. Org. Chem.*, **38**, 281 (2002).
[21] N.E. Jacobsen. *NMR Spectroscopy Explained*, pp. 186–187, John Wiley & Sons, Inc., Hoboken, New Jersey (2007).
[22] D. Sanz, A. Perona, R.M. Claramunt, J. Elguero. *Tetrahedron*, **61**, 145 (2005).
[23] K.K. Upadhyay, A. Kumar, S. Upadhyay, P.C. Mishra. *J. Mol. Struct.*, **873**, 5 (2008).
[24] G.-Y. Yeap, S.-T. Ha, N. Ishizawa, K. Suda, P.-L. Boey, W.A.K. Mahmood. *J. Mol. Struct.*, **658**, 87 (2003).
[25] T. Głowiak, L. Jerzykiewicz, J.M. Sobczak, J.J. Ziółkowski. *Inorg. Chim. Acta*, **356**, 387 (2003).
[26] K. Nakamoto. *Infrared and Raman Spectra of Inorganic and Coordination Compounds*, 4th Edn, John Wiley and Sons, Inc., New York (1986).
[27] D.L. Pavia, G.M. Lampman, G.S. Kriz, J.A. Vyvyan. *Introduction to Spectroscopy*, 4th Edn, Brooks Cole, Belmont, CA (2009).
[28] M. Sebastian, V. Arun, P.P. Robinson, P. Leeju, D. Varghese, G. Varsha, K.K.M. Yusuff. *J. Coord. Chem.*, **63**, 307 (2010).
[29] A.B.P. Lever. *Inorganic Electronic Spectroscopy*, 2nd Edn, Elsevier, Amsterdam (1984).
[30] W.C. Potter, L.T. Taylor. *Inorg. Chem.*, **15**, 1329 (1976).
[31] N.U. Shetty, V.K. Revankar, V.B. Mahale. *Proc. Indian Acad., Chem. Sci.*, **109**, 7 (1997).
[32] R.S. Drago. *Physical Methods in Inorganic Chemistry*, Rein Hold, New York, USA (1965).
[33] F.A. Cotton, G. Wilkinson, C.A. Murillo, M. Bochmann. *Advanced Inorganic Chemistry*, 6th Edn, Wiley, New York (1999).
[34] A.A. El-Asmy, G.A.A. Al-Hazmi. *Spectrochim. Acta A*, **71**, 1885 (2009).
[35] D. Kivelson, R. Neiman. *J. Chem. Phys.*, **35**, 149 (1961).
[36] I. Adato, A.H.I. Ben-Bassat, S. Sarel. *J. Phys. Chem.*, **75**, 3828 (1971).
[37] R. Pogni, M.C. Baratto, A. Diaz, R. Basosi. *J. Inorg. Biochem.*, **79**, 333 (2000).
[38] V. Arun, N. Sridevi, P.P. Robinson, S. Manju, K.K.M. Yusuff. *J. Mol. Catal. A: Chem.*, **304**, 191 (2009).